Supporting Information

Na₂MoO₂F₄:Mn⁴⁺ Phosphor with Red Luminescence Peaking at 625 nm and ZPL/v_6 Intensity Ratio of 243%

Qiao Qu, [a] Konglan Chen, [b] Yayun Zhou,*[b] Jinsheng Li, [c] and Haipeng Ji*[a]

[a]   School of Materials Science and Engineering, Zhengzhou University, Zhengzhou 450001, China

[b]   Guangdong-Hong Kong-Macao Joint Laboratory for Intelligent Micro-Nano Optoelectronic Technology, School of Physics and Optoelectronic Engineering, Foshan University, Foshan 528225, China

[c]   Key Laboratory of Dielectric and Electrolyte Functional Materials Hebei Province, School of Resources and Materials, Northeastern University at Qinhuangdao, Qinhuangdao 066004, China

Corresponding Authors

Yayun Zhou − orcid.org/0000-0002-0952-1481; Email: zhouyayun@fosu.edu.cn

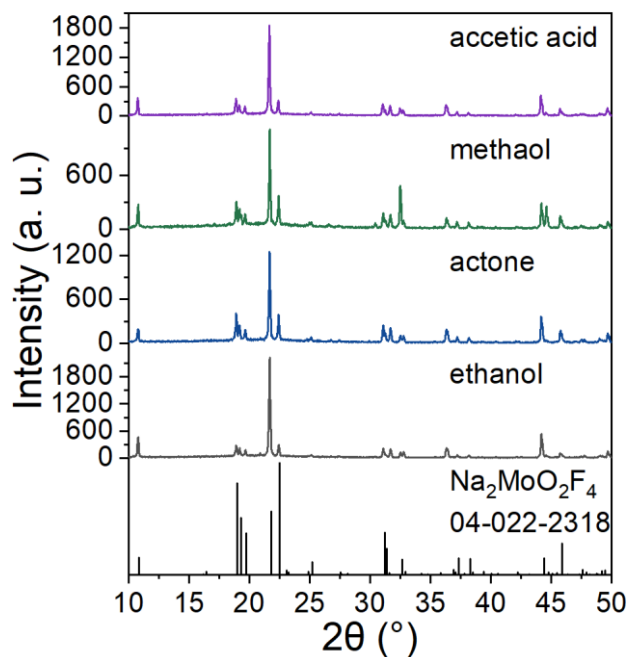Haipeng Ji − orcid.org/0000-0003-2585-5665; Email: jihp@zzu.edu.cn

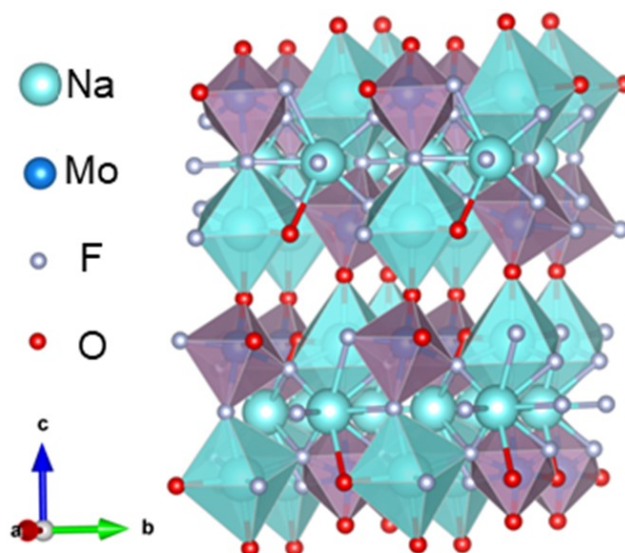**Figure S1** The XRD patterns of Na₂MoO₂F₄:1.5%Mn⁴⁺ phosphors with 5 mL organics.

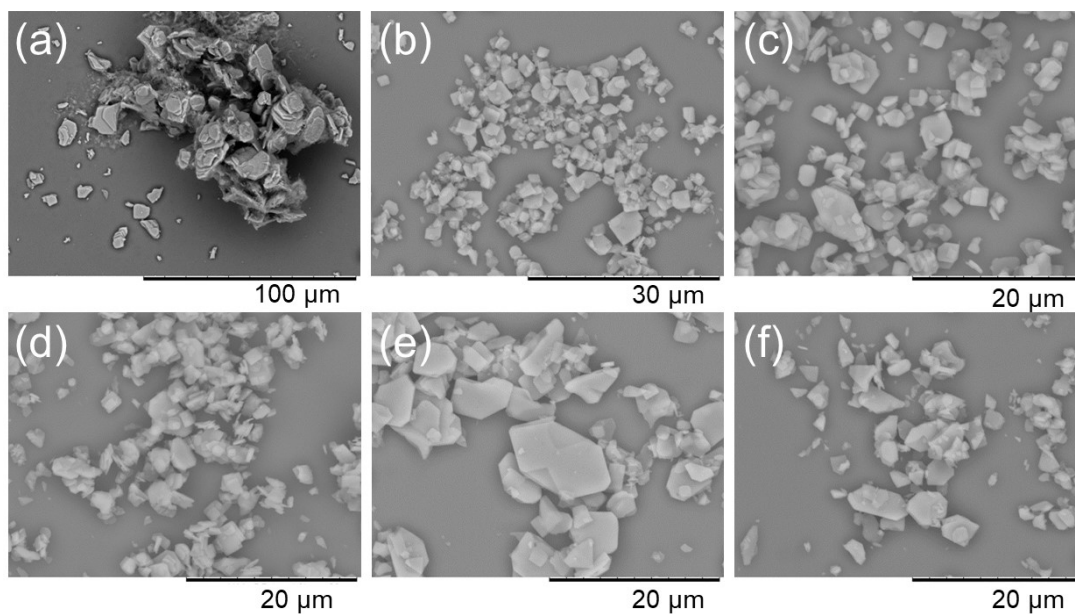**Figure S2** Crystal structure of $Na_2MoO_2F_4$ showing a $2 \times 2 \times 1$ supercell.

Figure S3 SEM images of $Na_2MoO_2F_4$ (a) and $Na_2Mo_{1-x}O_2F_4{:}x$Mn^{4+} (b~f correspond to $x =$ 0.3%, 0.6%, 1.0%, 1.5%, 2.0%, respectively).

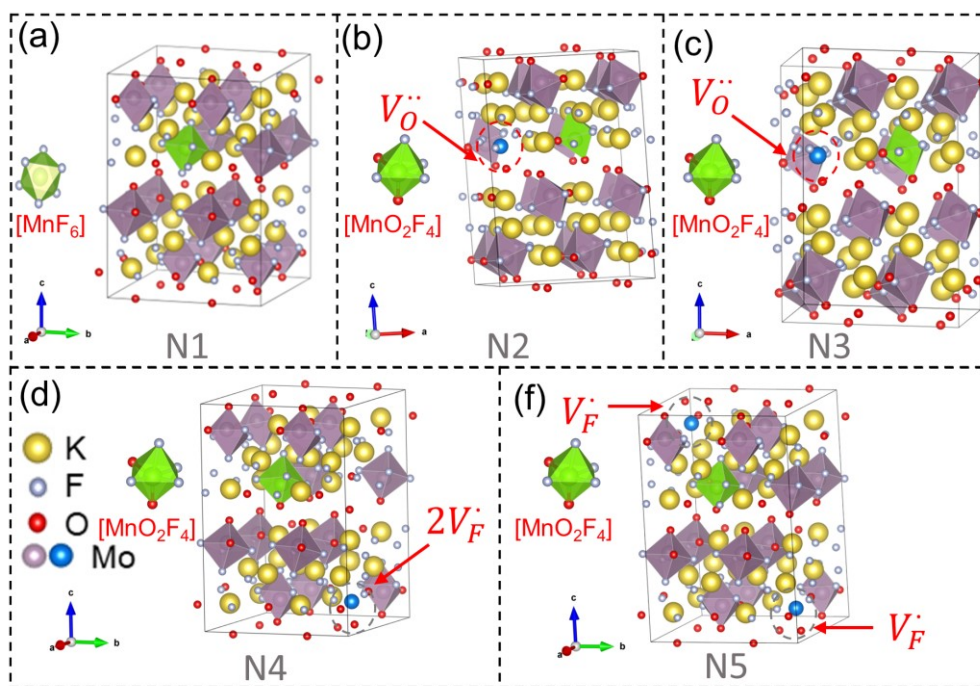**Figure S4** Five possible occupation forms and possible charge compensation models of Mn^{4+} or $[MnF_6]^{2-}$ doped in the $Na_2MoO_2F_4$ host.
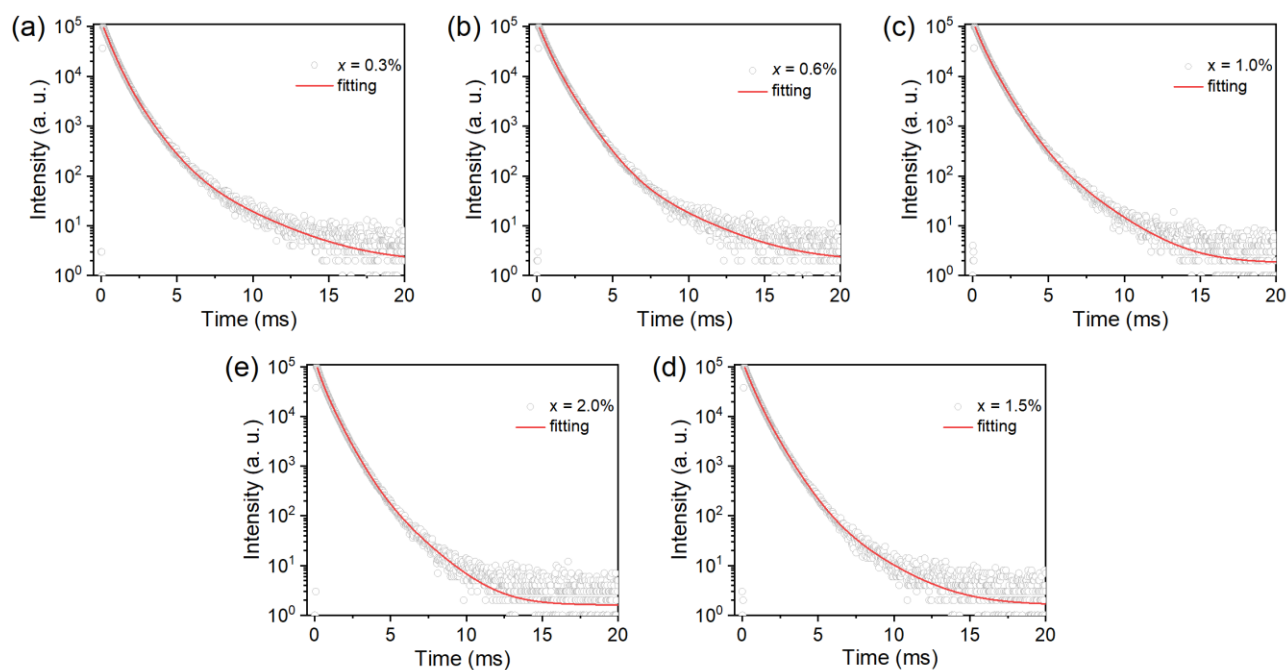
Figure S5 Luminescence decay curves of $Na_2Mo_{1-x}O_2F_4:xMn^{4+}$ phosphors, with x ranging from 0.3% to 2.0% (a~e correspond to x = 0.3%, 0.6%, 1.0%, 1.5%, 2.0%, respectively) monitored for 625 nm emission under 480 nm excitation.
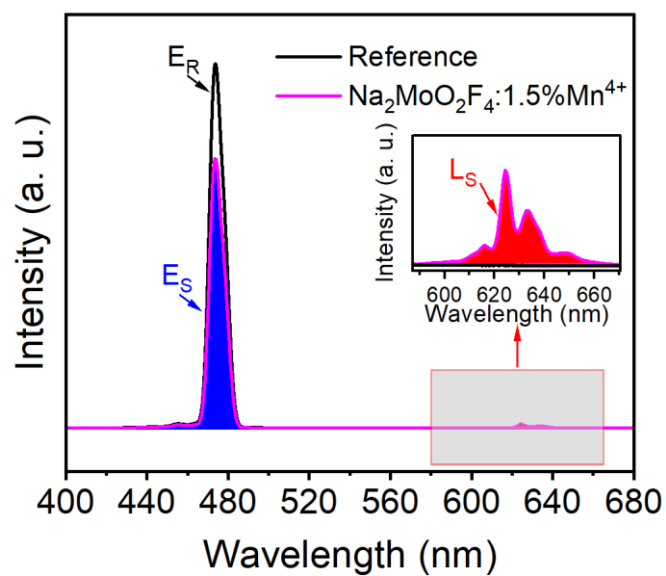
Figure S6. PL spectra (under 470 nm excitation) of $Na_2MoO_2F_4$:1.5%Mn^{4+} and reference

sample measured using an integrating sphere for quantum yield.
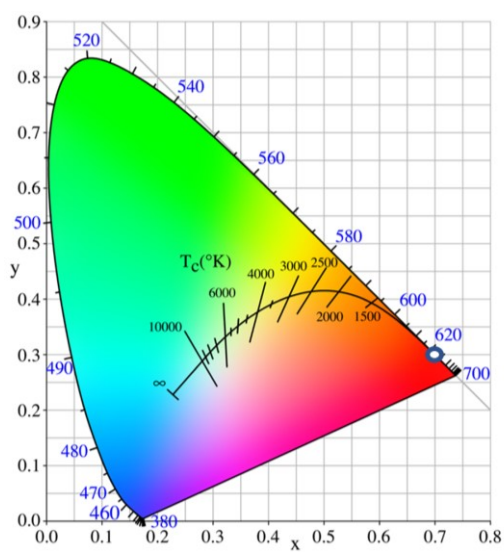
Figure S7. CIE chromaticity coordinate of $Na_2MoO_2F_4$:1.5%Mn^{4+} red phosphor.
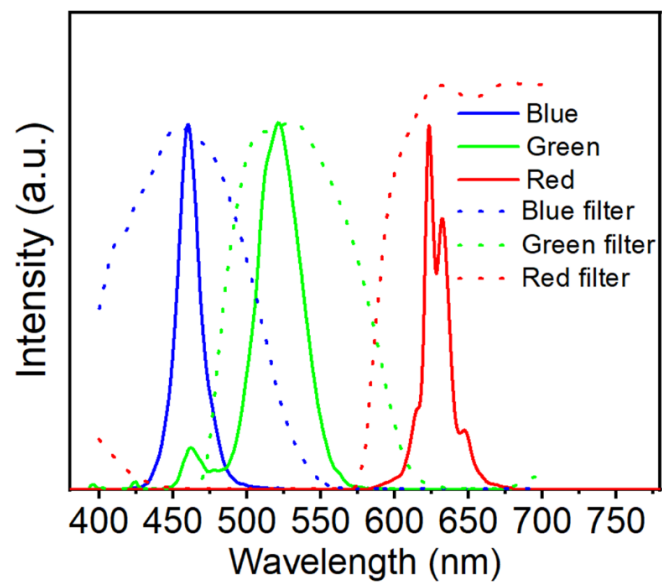
Figure S8. Transmission spectra of color filters (CFs) and RGB spectra of white LED after filtering by CFs.

Table S1 Yield of $Na_2MoO_2F_4$:1.5%Mn^{4+} treated by different amount of acetic acid

Usage (mL)	Yield
4	87.7%
5	89.9%
6	89.7%

Table S2 Crystallographic parameters of $Na_2MoO_2F_4$ from XRD Rietveld refinement

Items	Parameters
Space group	$P\,2_1/c$ (14)
Crystal structure	Monoclinic
a (Å)	5.50843
b (Å)	5.72113
c (Å)	16.40740
α (°)	90
β (°)	91.46095
γ (°)	90
Volume (Å³)	516.902106
Mo–O1 (Å)	1.72481(5)
Mo–O2 (Å)	1.77387(4)
Mo–F1 (Å)	2.20214(6)
Mo–F2 (Å)	2.08913(5)
Mo–F3 (Å)	1.94605(5)
Mo–F4 (Å)	1.91554(6)
F3–Mo–O1 (°)	166.6487(5)
F1–Mo–F4 (°)	158.9484(5)
F1–Mo–O1 (°)	93.4231(8)
F1–Mo–O2 (°)	99.984(2)
F1–Mo–F2 (°)	81.189(2)
F1–Mo–F3 (°)	84.8704(9)
F2–Mo–O1 (°)	90.3483(17)
F2–Mo–F3 (°)	76.3024(17)
F2–Mo–F4 (°)	80.167(3)
F3–Mo–O2 (°)	90.1127(17)
F3–Mo–F4 (°)	81.3004(15)
F4–Mo–O2 (°)	95.853(3)
F4–Mo–O1 (°)	96.3753(14)
O1–Mo–O2 (°)	103.2174(16)
R_{wp} (%)	9.76
R_p (%)	7.15
χ^2	3.375

Table S3 The calculated formation energy for the five possible charge compensation models of Mn^{4+} or $[MnF_6]^{2-}$ doped in $Na_2MoO_2F_4{:}Mn^{4+}$ (2×1×1)

| Model	Compounds	Replacement forms	Formation energy (eV)
N1	$Na_{32}Mo_{15}MnO_{31}F_{66}$	$[MnF_6]^{2-} \rightarrow [MoO_2F_4]^{2-}$	1.3353166
N2	$Na_{32}Mo_{15}MnO_{31}F_{64}$	$Mn^{4+} \rightarrow Mo^{6+} - [O1]^{2-}$	7.57662195
N3	$Na_{32}Mo_{15}MnO_{31}F_{64}$	$Mn^{4+} \rightarrow Mo^{6+} - [O2]^{2-}$	7.57613195
N4	$Na_{32}Mo_{15}MnO_{32}F_{62}$	$Mn^{4+} \rightarrow Mo^{6+} - 2F^-$	11.7330173
N5	$Na_{32}Mo_{15}MnO_{32}F_{62}$	$Mn^{4+} \rightarrow Mo^{6+} - 2F^-$	11.8512373

Table S4 The bond angles and bond lengths of $[MnF_6]^{2-}$ in optimized $Na_2MoO_2F_4{:}Mn^{4+}$

Bond angles		Bond lengths	
F1–Mn–F2	91.8161(0)°	Mn–F1	1.86478(0) Å
F1–Mn–F3	93.3196(0)°	Mn–F2	1.88076(0) Å
F1–Mn–F5	87.6277(0)°	Mn–F3	1.85207(0) Å
F1–Mn–F6	91.9649(0)°	Mn–F4	1.81428(0) Å
F2–Mn–F3	92.8185(0)°	Mn–F5	1.82007(0) Å
F2–Mn–F4	87.5813(0)°	Mn–F6	1.78747(0) Å
F2–Mn–F5	87.0029(0)°		
F3–Mn–F4	92.1307(0)°		
F3–Mn–F6	90.9532(0)°		
F4–Mn–F5	86.9212(0)°		
F4–Mn–F6	88.2754(0)°		
F5–Mn–F6	89.1596(0)°		

Table S5 The fluorescence lifetime and structure of typical Mn^{4+}-doped (oxy)fluoride phosphors.

Phosphors	Lifetime (ms)	ZPL	Structure	Space group	Conc.(mol %)	Ref.
$Na_2SiF_6:Mn^{4+}$	5.80	Strong	Trigonal	$D_3^2 - P321$	–	[1]
$K_2SiF_6:Mn^{4+}$	8.30	weak	Cubic	$O_h^5 - Fm\bar{3}m$	–	[2]
$K_3SiF_7:Mn^{4+}$	5.80	Weak	Tetragonal	P4/mbm	1	[3]
$Rb_2SiF_6:Mn^{4+}$	8.26	Weak	Cubic	$O_h^5 - Fm\bar{3}m$	–	[4]
$Rb_3SiF_7:Mn^{4+}$	5.38	Weak	Tetragonal	P4/mbm	1	[3]
$Cs_2SiF_6:Mn^{4+}$	7.81	Weak	Cubic	$O_h^5 - Fm\bar{3}m$	10.75	[5]
$Na_2GeF_6:Mn^{4+}$	6.58	Strong	Trigonal	$D_3^2 - P321$	<10	[6]
$K_2GeF_6:Mn^{4+}$	6.68	Weak	Trigonal	$D_{3d}^3 - P\bar{3}m1$	<3	[6]
$Rb_2GeF_6:Mn^{4+}$	6.02	Weak	Trigonal	$D_{3d}^3 - P\bar{3}m1$	<0.8	[6]
$Rb_2GeF_6:Mn^{4+}$	5.8	Strong	Hexagonal	$C_{6v}^4 - P63mc$	–	[7]
$Cs_2GeF_6:Mn^{4+}$	7.52	Weak	Cubic	$O_h^5 - Fm\bar{3}m$	<3	[6]
$K_2TiF_6:Mn^{4+}$	5.70	Weak	Trigonal	$D_{3d}^3 - P\bar{3}m1$	5.5	[8]
$Rb_2TiF_6:Mn^{4+}$	5.20	Weak	Trigonal	$D_{3d}^3 - P\bar{3}m1$	–	[9]
$Na_3AlF_6:Mn^{4+}$	4.68	Strong	Monoclinic	$C_{2h}^5 - P21/c$	1.58	[10]
$K_3AlF_6:Mn^{4+}$	3.50	Strong	Cubic	$O_h^5 - Fm\bar{3}m$	3.41	[11]
$K_2NaAlF_6:Mn^{4+}$	6.63	Strong	Cubic	$O_h^5 - Fm\bar{3}m$	2.03	[12]
$Cs_3AlF_6:Mn^{4+}$	2.83	Weak	Cubic	$O_h^5 - Fm\bar{3}m$	1.83	[13]
$K_2NaGaF_6:Mn^{4+}$	5.68	Strong	Cubic	$O_h^5 - Fm\bar{3}m$	–	[14]
$K_2NbF_7:Mn^{4+}$	3.62	Strong	Monoclinic	$C_{2h}^5 - P21/c$	<1	[15]
$KTeF_5:Mn^{4+}$	3.29	Medium	Orthorhombic	$D_{2h}^{11} - Pbcm$	0.23	[16]
$Na_2WO_2F_4:Mn^{4+}$	2.59	Strong	Orthorhombic	$D_{2h}^{14} - Pbcn$	0.5	[17]
$LiAl_4O_6F:Mn^{4+}$	0.24~3.5	–	Cubic	–	–	[18]
$LiNaWO_2F_4:Mn^{4+}$	1.21	Strong	Orthorhombic	$D_{2h}^{14} - Pbcn$	2	[19]
$KNaWO_2F_4:Mn^{4+}$	2.02	Strong	Orthorhombic	$D_{2h}^{14} - Pbcn$	4	[19]
$Rb_2WO_2F_4:Mn^{4+}$	2.15	Weak	Trigonal	$D_{3d}^3 - P\bar{3}m1$	11	[20]
$Cs_2WO_2F_4:Mn^{4+}$	3.2	Weak	Trigonal	$D_{3d}^3 - P\bar{3}m1$	5	[21]
$K_3WOF_7:Mn^{4+}$	–	Medium	Monoclinic	$C_{2h}^5 - P21/c$	–	[22]
$K_2[MoO_2F_4] \cdot H_2O:Mn^{4+}$	3.78	Medium	Monoclinic	$C_{2h}^5 - P21/c$	3.28	[23]
$Cs_2MoO_2F_4:Mn^{4+}$	1.95	Medium	Orthorhombic	Amam	1.12	[24]
$Rb_2MoO_2F_4:Mn^{4+}$	3.66	Medium	Orthorhombic	Amam	5	[25]
$CsMoO_2F_3:Mn^{4+}$	1.88	Weak	Orthorhombic	$D_{2h}^{28} - Imma$	3.88	[26]
$Cs_2NbOF_5:Mn^{4+}$	3.23	Weak	Trigonal	$C_3^1 - P3$	6.98	[27]
$Rb_2NbOF_5:Mn^{4+}$	4.73	Weak	Trigonal	$C_3^1 - P3$	1	[28]
$Na_2NbOF_5:Mn^{4+}$	3.32	Strong	Orthorhombic	Pbcn(60)	0.3	[29]
$BaNbOF_5:Mn^{4+}$	–	Strong	Cubic	$T_h^6 - Pa\bar{3}$	6	[30]
$K_3TaO_2F_4:Mn^{4+}$	4.24	Medium	Cubic	$O_h^5 - Fm\bar{3}m$	6.92	[31]

Table S6 The CIE1931 color coordinates of the red, green and blue components of this WLED incorporating β-SiAlON:Eu^{2+}, Na$_2$MoO$_2$F$_4$:1.5%Mn^{4+} phosphor, and an InGaN chip at 20 mA current

CIE	White	Red	Green	Blue
x	0.295	0.673	0.141	0.141
y	0.313	0.292	0.683	0.039

Calculation for crystal field strength and Racah parameters:

The crystal-field strength (Dq) of Mn^{4+} can be roughly estimated by the peak energy of $^4A_{2g}\rightarrow^4T_{2g}$ transition[32]:

$$Dq = E(^4A_{2\mathrm{g}} \rightarrow^4 \mathrm{T_{2g}})/10$$

Based on the peak energy difference between $^4A_{2g}\rightarrow^4T_{1g}$ and $^4A_{2g}\rightarrow^4T_{2g}$, the Racah parameter B can be calculated by the following equation[32]:

$$\frac{Dq}{B} = \frac{15(x-8)}{(x^2-10x)}$$

where the parameter x is defined as

$$x = \frac{E(^4A_{2g} \rightarrow^4 T_{1g}) - E(^4A_{2g} \rightarrow^4 T_{2g})}{Dq}$$

According to the peak energy for Mn^{4+}: $^2E_g\rightarrow^4A_{2g}$ transition, the Racah parameter C is evaluated by the following equation {Henderson, 1989 #1015}:[32]

$$\frac{E(^2E_g \rightarrow^4 A_{2g})}{B} = \frac{3.05C}{B} - \frac{1.8B}{Dq} + 7.9$$

Calculation for IQE, AE and EQE:

The internal quantum efficiency (IQE), absorption efficiency (AE) and external quantum efficiency (EQE) of the Na$_2$MoO$_2$F$_4$:1.5%Mn^{4+} were measured to be 7.6%, 26.29% and 2%, respectively. The IQE (termed as η_{int}) was calculated by using the following equation :[33]

$$\eta_{int} = \frac{\int L_S}{\int E_R - \int E_S}$$

where L_S is the emission spectrum of the sample, and E_S and E_R stand for the excitation spectra of the excitation light used for exciting the sample and without the sample in the integrating sphere, respectively. The AE of the sample, ε_{abs}, was calculated via the expression:

$$\varepsilon_{abs} = \frac{\int E_R - \int E_S}{\int E_R}$$

The EQE (η_{ext}) was determined via the equation:

$$\eta_{ext} = \varepsilon_{abs} \times \eta_{int}$$

Reference

1 H.D. Nguyen, C. C. Lin, M.H. Fang and R.S. Liu, *J. Mater. Chem. C*, 2014, **2**, 10268–10272.

2 J. W. Moon, B. G. Min, J. S. Kim, M. S. Jang, K. M. Ok, K.Y. Han and J. S. Yoo, *Opt. Mater. Express*, 2016, **6**.

3 M. Kim, W. B. Park, J.W. Lee, J. Lee, C. H. Kim, S. P. Singh and K.-S. Sohn, *Chem. Mater.*, 2018, **30**, 6936–6944.

4 M.-H. Fang, H.D. Nguyen, C. C. Lin and R.S. Liu, *J. Mater. Chem. C*, 2015, **3**, 7277–7280.

5 E. Song, Y. Zhou, X. Yang, Z. Liao, W. Zhao, T. Deng, L. Wang, Y. Ma, S. Ye and Q. Zhang, *ACS Photonics*, 2017, **4**, 2556–2565.

6 H. Lian, Q. Huang, Y. Chen, K. Li, S. Liang, M. Shang, M. Liu and J. Lin, *Inorg. Chem.*, 2017, **56**, 11900–11910.

7 S. Sakurai, T. Nakamura and S. Adachi, *Jpn. J. Appl. Phys.*, 2018, **57**.

8 H. Zhu, C. C. Lin, W. Luo, S. Shu, Z. Liu, Y. Liu, J. Kong, E. Ma, Y. Cao, R. S. Liu and X. Chen, *Nat. Commun.*, 2014, **5**, 4312.

9 S. Sakurai, T. Nakamura and S. Adachi, *ECS J. Solid State Sci Technol.*, 2016, **5**, R206–R210.

10 E. H. Song, J. Q. Wang, S. Ye, X. F. Jiang, M. Y. Peng and Q. Y. Zhang, *J. Mater. Chem. C*, 2016, **4**, 2480–2487.

11 E. Song, J. Wang, J. Shi, T. Deng, S. Ye, M. Peng, J. Wang, L. Wondraczek and Q. Zhang, *ACS Appl Mater Interfaces*, 2017, **9**, 8805–8812.

12 L. Y. Wang, E. H. Song, T. T. Deng, Y. Y. Zhou, Z. F. Liao, W. R. Zhao, B. Zhou and Q. Y. Zhang, *Dalton Trans.*, 2017, **46**, 9925–9933.

13 H. Ming, L. Liu, S. He, J. Peng, F. Du, J. Fu, F. Yang and X. Ye, *J. Mater. Chem. C*, 2019, **7**, 7237–7248.

14 C. Jiang, M. G. Brik, L. Li, L. Li, J. Peng, J. Wu, M. S. Molokeev, K.-L. Wong and M. Peng, *J. Mater. Chem. C*, 2018, **6**, 3016–3025.

15 H. Lin, T. Hu, Q. Huang, Y. Cheng, B. Wang, J. Xu, J. Wang and Y. Wang, *Laser Photonics Rev.*, 2017, **11**.

16 T. T. Deng, E. H. Song, J. Su, Y. Y. Zhou, L. Y. Wang, S. Ye and Q. Y. Zhang, *J. Mater. Chem. C*, 2018, **6**, 4418–4426.

17 T. Hu, H. Lin, Y. Cheng, Q. Huang, J. Xu, Y. Gao, J. Wang and Y. Wang, *J. Mater. Chem. C*, 2017, **5**, 10524–10532.

18 N. Khaidukov, M. Brekhovskikh, G. Toci, B. Patrizi, M. Vannini, A. Pirri and V. Makhov, *J. Lumin.*, 2019, **216**, 116754–116754.

19 M. Hu, Z. Liu, Y. Xia, G. Zhang, Y. Fang, Y. Liu, G. Zhao and J. Hou, *J. Mater. Sci. Mater. Electron.*, 2020, **31**, 4535–4541.

20 S. Tang, Y. Liu, H. Li, Q. Zhou, K. Wang, H. Tang and Z. Wang, *J. Lumin.*, 2020, **224**,

117291–117291.

21 P. Cai, L. Qin, C. Chen, J. Wang and H. J. Seo, *Dalton Trans.*, 2017, **46**, 14331–14340.

22 C. Stoll, G. Heymann, M. Seibald, D. Baumann and H. Huppertz, *J. Fluorine Chem.*, 2019, **226**.

23 Y. Liu, H. Li, S. Tang, Q. Zhou, K. Wang, H. Tang and Z. Wang, *Mater. Res. Bull.*, 2020, **122**.

24 S. He, L. Yao, W. Cai, D. Wu, J. Peng and X. Ye, *Dalton Trans.*, 2020, **49**, 11290–11299.

25 Y. Zhou, H. Ming, S. Zhang, T. Deng, E. Song and Q. Zhang, *Chem. Eng. J.*, 2021, **415**, 128974.

26 S. He, F. Xu, T. Han, Z. Lu, W. Wang, J. Peng, F. Du, F. Yang and X. Ye, *Chem. Eng. J.*, 2020, **392**, 123657–123657.

27 J. Zhou, Y. Chen, C. Jiang, B. Milićević, M. S. Molokeev, M. G. Brik, I. A. Bobrikov, J. Yan, J. Li and M. Wu, *Chem. Eng. J.*, 2021, **405**.

28 Z. Wang, Z. Yang, Z. Yang, Q. Wei, Q. Zhou, L. Ma and X. Wang, *Inorg. Chem.*, 2019, **58**, 456–461.

29 J. Hou, W. Yin, L. Dong, Y. Li, Y. Liu, Z. Liu, G. Zhao, G. Zhang and Y. Fang, *Materials (Basel, Switzerland)*, 2021, **14**.

30 X. Dong, Y. Pan, D. Li, H. Lian and J. Lin, *CrystEngComm*, 2018, **20**, 5641–5646.

31 Y. Zhou, S. Zhang, X. Wang and H. Jiao, *Inorg. Chem.*, 2019, **58**, 4412–4419.

32 B. Henderson and G. F. Imbusch, *Optical spectroscopy of inorganic solids*, Oxford University Press, 2006.

33 Q. Dong, P. Xiong, J. Yang, Y. Fu, W. Chen, F. Yang, Z. Ma and M. Peng, *J. Alloys Compd.*, 2021, **885**, 160960.